Mechanism of Disc Rupture
A Preliminary Report

STUART J. GORDON, MD,* KING H. YANG, PhD,† PHILIP J. MAYER, MD,* ANDREW H. MACE, Jr., MD,‡ VINCENT L. KISH,* and ERIC L. RADIN, MD*

Lumbar intervertebral disc herniation is thought to be related to senescent changes in the nucleus pulposus except in rare instances of trauma. This investigation provides the first *in vitro* model of disc prolapse that reliably ruptures discs under physiologically reasonable stress. Fourteen vertebral motion segments with intact posterior elements were loaded repetitively at 1.5 Hz in a combination of flexion (7°), rotation (< 3°), and compression (1,334 N) for an average of 6.9 hours (range, 3.0–13.0 hours) in a materials testing machine. Loading was terminated when reaction force leveled off for more than 1 hour. Ten discs failed through annular protrusions, and four failed by nuclear extrusion through annular tears, supporting the hypothesis that intervertebral disc prolapse is peripheral in origin. The annulus fibrosus is the site of primary pathologic change. [Key words: disc prolapse, *in vitro*, annulus]

MANY HAVE INVESTIGATED the unique properties of the intervertebral disc and suggested its physiology and pathophysiology. Early studies attempted to produce prolapse with static loads in compression. Several investigators found end-plate failure before any evidence of disc injury.[6,9,11,23,24,27] Failure loads were documented between 1,570 and 5,880 N.[11] Farfan et al[10] pioneered rotation as a mechanism, yet produced only annular tears without prolapse. He observed that annular injury occurred when rotation exceeded 3°, a value later confirmed mathematically by Hickey and Hukins.[15] Other investigators observed that flexion at 9° or greater led to supraspinous and interspinous ligament injury[1]—or vertebral body fracture[24]—but not disc injury.

Based on these observations and the clinical knowledge that many, if not most, prolapsed discs do not have a significant history of trauma, several studies investigated multiaxial loading in both static and dynamic modes. Liu et al[18] did not produce prolapse through a combination of repetitive rotation and compression. Adams and Hutton's[2] landmark work reported the first production of annular protrusion and nuclear extrusion by a static combination of axial compression and hyperflexion. The degree of flexion used, however, was not physiologic in humans.[4] Follow-up investigation by these authors using less flexion and a cycled axial load did not produce prolapse in dye-injected discs. Only when the flexion angle and axial compression were increased beyond physiologic loads did they obtain positive findings.[3] An investigation by Anderson et al[5] found that nuclear injection significantly altered the biomechanical properties of disc.

Preliminary work by Yang et al[28] in our laboratories produced external annular tears and nuclear extrusion by a physiologically reasonable combination of cyclic flexion, compression, and rotation. Although this investigation provided the first confirmation that disc prolapse could be caused by this combination, an idea shared by others,[11,15,17,24] it sacrificed the posterior elements to detect intervertebral damage. We believed it was necessary to repeat the experiment with retention of the posterior elements using magnetic resonance imaging (MRI) to evaluate the pre- and posttest status of the discs. This preliminary report shows the results of the first 14 motion segments studied.

MATERIALS AND METHODS

Block specimens of human spine from the lower thoracic region to the sacrum were obtained from the Human Gift Registry of West Virginia University Hospital. Specimens were used immediately or kept frozen at −20 C and thawed just before testing, a storage technique known not to alter significantly the material properties of test tissues.[13,22,26] Plain radiographs of the block spines were obtained. The MRI was done in a General Electric (Milwaukee, WI) Signa 1.5 T machine. The slice thickness was 5 mm with a 1-mm skip region. Sagittal views were obtained at a time to echo/time to repetition (TE/TR) of 20/500 and 20/2,500 or 80/2,500 and axial views at a TE/TR of 20/2,500 or 80/2,500. Pre-existing degenerative changes were blindly graded at each disc level using the plain radiographs (Table 1) and MRI (Table 2) by a staff radiologist (AHM) and a staff spine surgeon (PJM). Intervertebral levels showing Schneiderman's Grade 3 or 4 degenerative changes by plain radiography or MRI criteria[25]—or the presence of prolapse on axial or sagittal views by MRI—were rejected.

Vertebral motion segments containing the intervertebral disc and the complete superior and inferior vertebra were formed. All soft tissue except the anterior longitudinal ligament, posterior longitudinal ligament, ligamentum flavum, facet capsules, supraspinous ligament, and interspinous ligament were removed. In addition MRI compatible brass screws were placed in the superior end of the superior body and the inferior end of the inferior body to aid potting fixation. Motion segments were potted using polymethylmethacrylate (DUZALL, Coralite Dental Products, Skokie, IL) in two shallow potting cups with the center of the disc aligned with the center of the upper cup. A special jig was used to ensure that the superior and inferior end-plates were parallel to the cups to prevent induction of a flexion or extension moment.

Potted motion segments were placed on a materials testing machine (Model 410, MTS Systems Corporation, Minneapolis, MI) and packed with saline-soaked gauze sponges to prevent dehydration (Figure 1). Segments were first loaded in pure compression to obtain axial stress relaxation data. After the initial load of 226 N was achieved, displacement was maintained at that level for 30 minutes. Two segments had postrelaxation radiographs and MRI to confirm that no change had been induced by this preconditioning process.

Motion segments were then flexed 7° from neutral by goniometer measurement. Using a load-control mode, 1,334 N of axial compression was generated. The initial loading displacement at this level was recorded. The testing device was then changed to a displacement-

From the *Department of Orthopedic Surgery and the ‡Department of Radiology, West Virginia University, Morgantown, West Virginia, and the †Department of Mechanical Engineering, Orthopedic Surgery and Bioengineering Center, Wayne State University, Detroit, Michigan.
Submitted for publication November 19, 1989, and revised September 28, 1990.
The authors thank Donna Morris for MRI technical assistance, David Burr, PhD, for providing specimens, and Jeanne Grimm for editorial assistance.

Table 1. Radiographic Degenerative Grade

Grade	Degree of Degeneration
1	Normal (no sclerosis, narrowing, or osteophytes)
2	Minimal (minimal sclerosis narrowing, or minor osteophytes)
3	Moderate (moderate sclerosis, narrowing, or osteophytes)
4	Severe (severe sclerosis, narrowing, or osteophytes)

Table 2. MRI Degenerative Grade[25]

Grade	MRI Signal	Definition
1	Normal	Normal height and signal intensity
2	Intermediate	Speckled pattern or heterogeneous decrease
3	Marked	Diffuse loss of signal
4	Absent	Signal void

control mode to load the specimen to the initial load displacement at each cycle. This sequence allowed us to load the spine to a normal standing posture and to take into account the viscoelastic nature of the disc. The change to displacement-control mode avoided the generation of excessive axial displacements and rotation. A fixture incorporated into the MTS machine converted axial displacement into counterclockwise rotation.

The amount of rotation depended on the axial displacement and rotational stiffness of the specimen but always remained at or below 3°. The segment was loaded at 1.5 Hz half-triangular wave form. Force dropoff was followed continuously with load-displacement curves recorded initially and every 30 minutes thereafter. Testing was completed when force decrement showed evidence of an asymptotic nature. After termination of loading, follow-up radiographs of the motion segment were obtained to evaluate the possibility of end-plate or vertebral body failure. Follow-up MRI was done as described above.

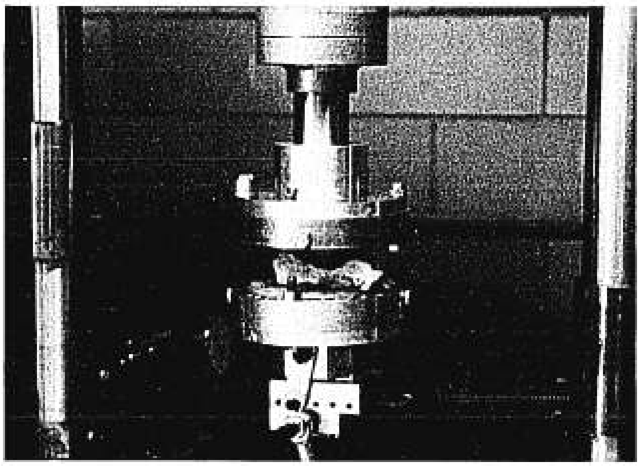

Fig 1. Potted motion segment loaded onto a materials testing machine. The inferior jig converts axial displacement to counterclockwise rotation. Saturated gauze sponges are used to prevent dehydration.

Intervertebral disc prolapse was blindly assessed by MRI and gross examination based on definitions presented by Adams and Hutton.[2] Nuclear extrusion was shown by a complete radial fissure between the central nucleus and an intact or disrupted annulus (Figure 2). This was determined by comparison of pre- and postload axial MRI images and later confirmed by comparison with gross transverse disc sections. Annular protrusion was defined as a change in the morphology of this portion of the disc as witnessed by comparison of pre- and postload axial and sagittal MRI images (Figure 3).

Posterior elements were observed for damage, then removed, allowing more complete examination of the posterior disc. Finally, discs were sectioned transversely, graded according to the classification of Galante[13] (Table 3), and categorized by either the presence of nuclear extrusion or annular protrusion.

Biomechanical assessment of the force-deformation data curves was done. Motion segments were reviewed with respect to combinational stiffness and energy loss. Data were analyzed statistically using the Mann-Whitney U test and the Fisher exact probability test, where appropriate.

RESULTS

Fourteen discs from nine spines met our imaging criteria (Table 4) with four discs each at the L1–2, L3–4, and L4–5 levels and two at the L2–3 level. The average specimen age was 57 years (range, 18–65 years); all were from white men. A medical history concerning prior spinal complaints was unavailable.

On gross examination, ten discs showed annular protrusion (one bilateral), and four showed nuclear extrusion (Table 5). Annular tears were found in all specimens in the posterolateral region, either associated with annular protrusion (Figure 4) or adjacent to the radial fissure of a nuclear extrusion. These tears were discernible on sagittal MRI views as disruptions of the posterior annulus and on axial views as signalless spaces on T2-weighted imaging. Correlation between gross and MRI findings was 69% (11 of 14) overall, 90% (9 of 10) for annular protrusion, and 50% (2 of 4) for nuclear extrusion.

Seven motion segments showed no plain radiographic evidence of degenerative change; seven showed minimal change. None of these plain radiographic grades changed after loading. One segment had an anterior compression fracture of the superior body. Discs that resulted in nuclear extrusion showed a statistically significant ($P = 0.035$) association with Grade 2 radiographic degeneration over the annular protrusion discs more often than Grade 1 (seven of ten). Comparison of Galante grading between the two groups was not statistically significant.

Table 6 shows displacements used in the stress–relaxation test and loading parameters used in subsequent combination-loading experiments. Average rotation, always in a counterclockwise rotation, was 1.9°. The average duration of testing was 36,750 cycles, or 408 minutes (6.9 hours; range, 181–780 minutes). No particular disc extrusion pattern was found to correlate with the initial biomechanical parameters.

Biomechanical data (Tables 7–10) were available for nine discs, three with nuclear extrusion and six with annular protrusion. No significant statistical difference was observed for either subset with respect to combinational loading stiffness measured at the end stage of the load-deformation curve. Again, no significant difference was observed. Energy loss calculated (Table 11) from hysteresis curves showed no difference between extrusion and protrusion specimens.

DISCUSSION

This preliminary work presents the first *in vitro* model for intervertebral disc prolapse based on a physiologically reasonable loading pattern. We used a combination of flexion, compression, and rotation. Our hypothesis emphasizes the role of environment in producing

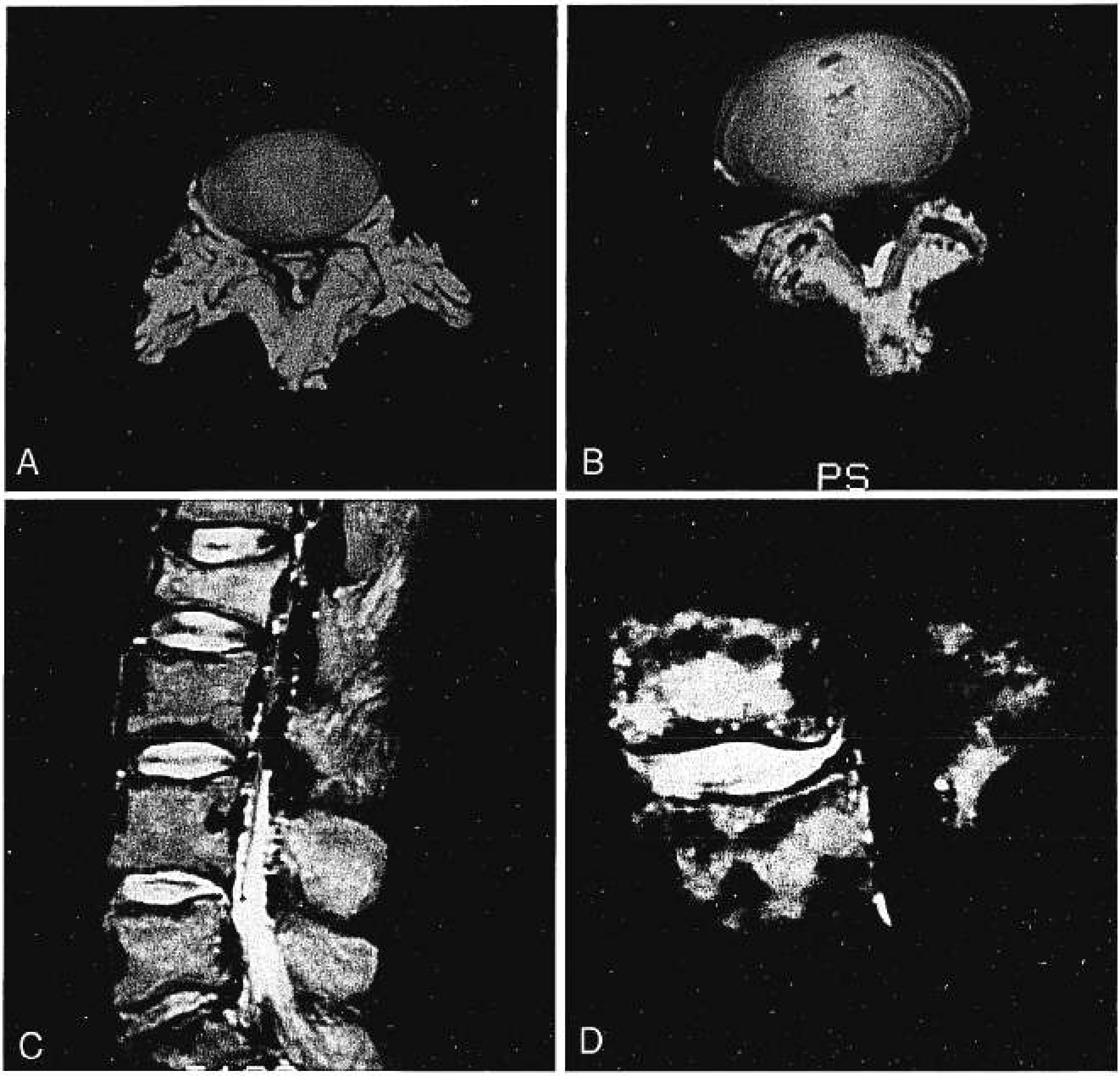

Fig 2. A, Segment 1. Preload axial T1-weighted image. **B**, Postload, note central extrusion. **C**, Preload sagittal T2-weighted image. Note intact posterior annulus. **D**, Postload. Note nuclear extrusion with annular disruption. This sagittal plane is in the midline. **E**, Gross examination. Note central extrusion with disrupted posterior annulus.

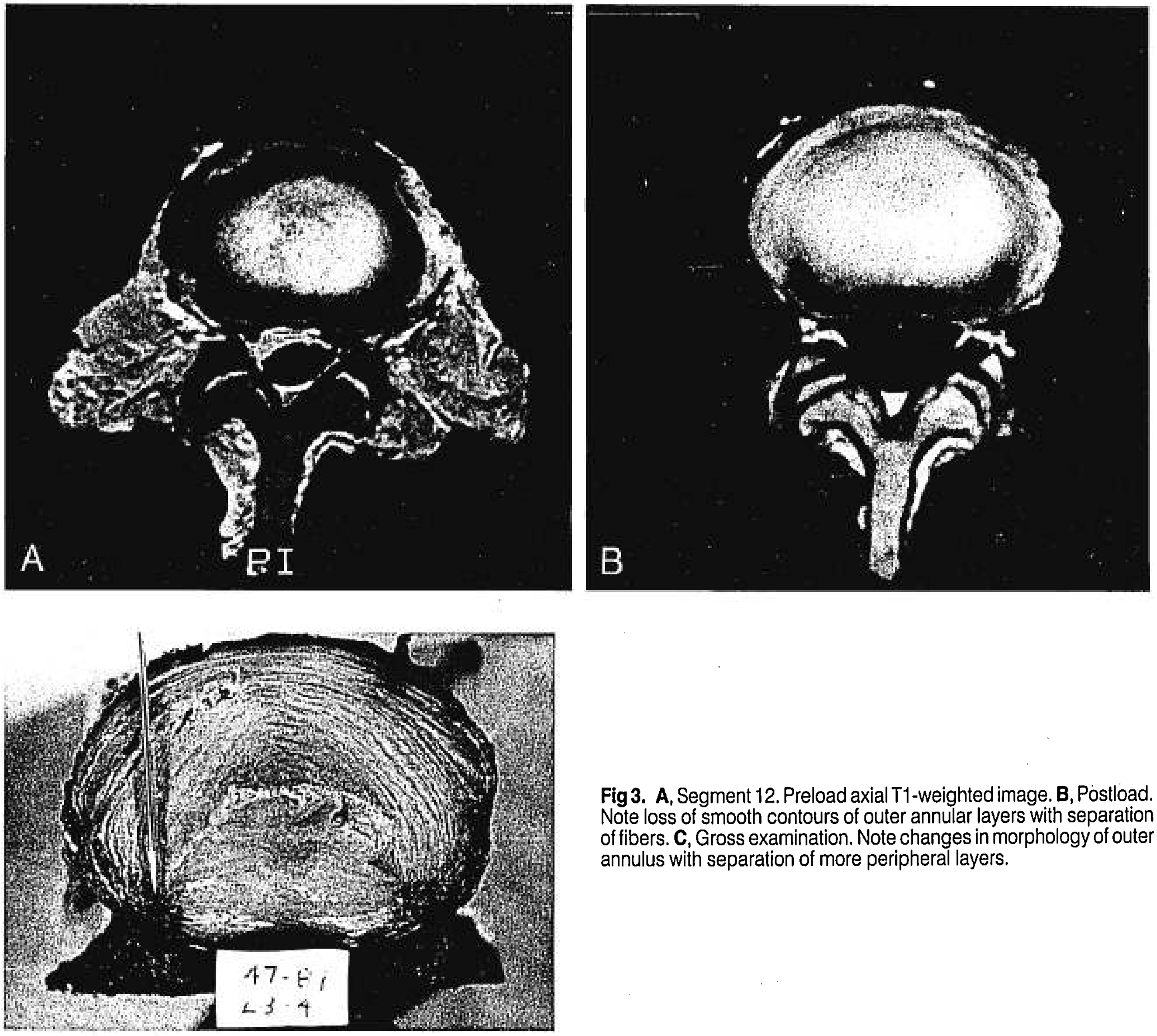

Fig 3. A, Segment 12. Preload axial T1-weighted image. **B,** Postload. Note loss of smooth contours of outer annular layers with separation of fibers. **C,** Gross examination. Note changes in morphology of outer annulus with separation of more peripheral layers.

Table 3. Galante Grade[13]

1	Normal discs. Annulus free from ruptures and shiny white.
2	The appearance is normal, but the nucleus exhibits a more fibrous structure. A clear boundary is present between annulus and nucleus.
3	Isolated fissures in the annulus. The nucleus is dry and occasionally discolored. The boundary between the nucleus and the annulus is no longer distinct.
4	Severe changes. Ruptures and sequestrae in both the annulus and nucleus. Marginal osteophytes found.

Table 4. Segment Biologic Data

Segment	*Spine*	*Level*	*Age*	*Cause of Death*
1	1	45	60	Cardiopulmonary arrest
2	2	23	63	Natural
3	2	45	63	Natural
4	3	12	64	Cardiopulmonary arrest
5	3	45	64	Cardiopulmonary arrest
6	4	12	18	Fall
7	4	34	18	Fall
8	5	34	68	Ruptured AAA
9	6	12	63	Pulmonary emboli
10	6	34	63	Pulmonary emboli
11	7	12	62	Respiratory arrest
12	8	34	65	CHF
13	9	23	65	Alcoholism
14	9	45	65	Alcoholism

AAA = abdominal aortic aneurysm; CHF = congestive heart failure.

Table 5A. Stress-Relaxation

Segment	Application (S)	Displacement (mm)
1	NA	NA
2	0.6	0.05
3	NA	0.20
4	0.6	0.43
5	0.4	0.30
6	0.8	0.18
7	NA	0.15
8	0.5	0.36
9	0.6	0.46
10	0.7	0.41
11	1.0	0.25
12	0.5	0.30
13	0.5	0.30
14	0.5	0.46

NA = not available.

Table 5B. Combination-Loading

Displacement (mm)	Flexion(°)	Rotation(°)	Compression (N)	Cycle
2.24	7	2.9	1334	30720
0.53		2.5		34070
0.61		2.3		40500
1.09		2.0		70200
0.53		1.0		28420
0.76		1.5		32400
0.71		2.0		33250
0.86		2.0		53580
0.74		1.5		42480
0.66		1.3		32330
0.76		1.5		33170
0.64		1.5		34800
0.74		1.5		32290
2.16		3.0		16290

prolapse and supports the frequent absence of trauma in clinical history. Dandy[8] recognized this as early as 1929. The use of MRI allowed us to maintain the posterior elements while assessing pre-and postdisc status. Correlation between gross and MRI findings was generally high; however MRI had limitations, ie, the nucleus and annulus were indistinguishable in the sagittal plane. Therefore, any attempt to specify nuclear injury in this plane based on MRI without the benefit of gross observation is unreliable. As in previously published work,[7,19,21] we observed that sagittal views were generally more sensitive than axial views in detecting prolapse. Although MRI was useful in predicting preload degenerative status and postload morphologic changes of the disc, comment on the effect of multiple loads on the MRI signal is not possible. The preload MRI disc signal was based on images from a block specimen and was used to identify acceptable segments. The postload disc signal reflected only the involved motion segments. Although comparison for prolapse is possible because this is a morphologic evaluation, the difference in the amount of soft tissue leading to the production of preload and postload signals would make any comparative comment invalid. This narrower field might subtly influence the MRI signals, but the predominant image evoked is from the anatomic structure. For this reason, we did not depend totally on the MRI signals to define annulus damage or disc herniation.

In our study, lumbosacral segments were rejected uniformly by the MRI determination of disc status. Although the average age of specimens in this study was slightly higher than the peak years of prolapse,[16] our selection process provided a relatively young group of discs. All

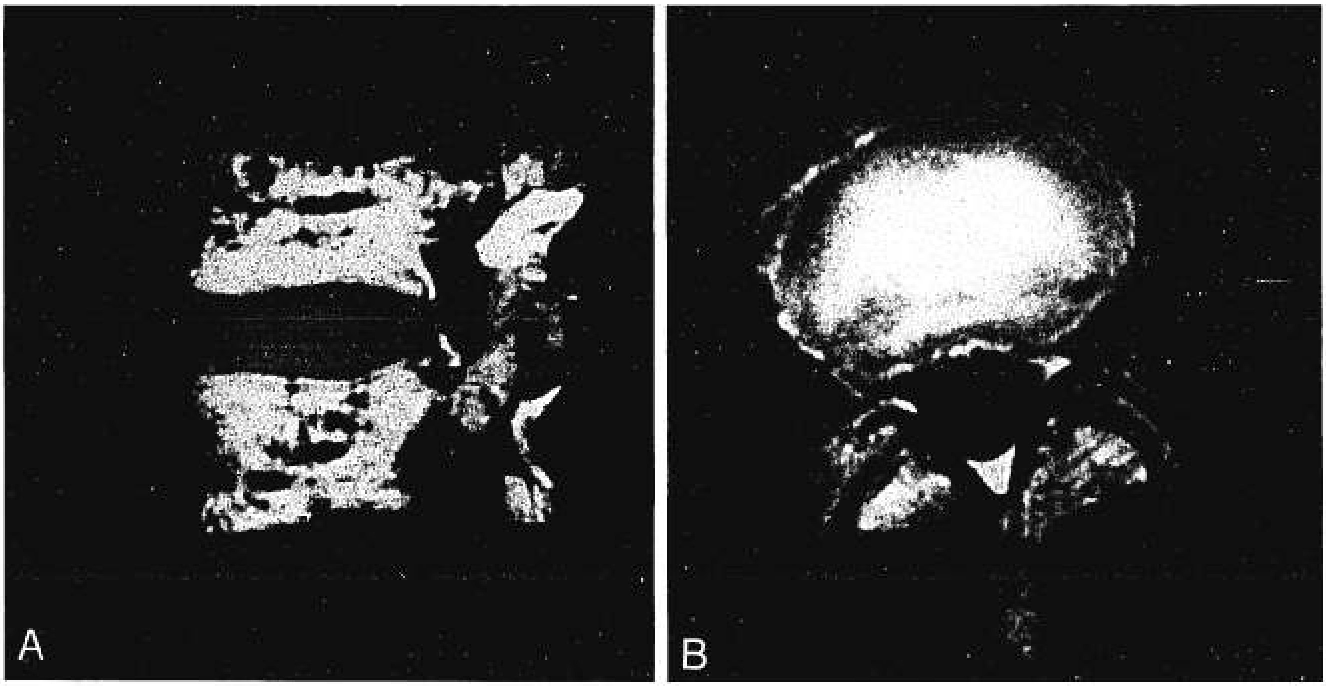

Fig 4. A, Annular tear, sagittal view. Note disruption of annulus at posteroinferior region. **B,** Annular tear, axial view. Note signalless space.

Table 6. Radiologic Data

	Gross Findings				Radiography		MRI	
Segment	AP	NE	AT	GAL	Preop	Postop	AP	NE
1		Central	+	2	2	2		+
2	R		+	2	1	1	+	
3	L		+	2	1	1	+	
4	L		+	3	1	1	+	
5	R		+	3	2	2	+	
6	L		+	1	2	2	−	
7	R		+	1	1	1	+	
8	L		+	3	2	2		−
9	R		+	3	2	2		−
10	BIL		+	3	1	1	+	
11	R		+	3	2	2		+
12	L		+	3	1	1	+	
13	L		+	2	1	1	+	
14*	L		+	2	2	2	+	

*Anterior compression fracture of superior body.
AP = annular protrusion; NE = nuclear extrusion; AT = annular tear; GAL = Galante grade; BIL = bilateral.

motion segments were derived from white men, a limitation imposed by spine availability. Previously published data support the general application of our findings.[20]

After excluding significantly degenerated discs by imaging criteria, mildly degenerated discs by plain radiographic criteria appeared more often associated with nuclear extrusion than undegenerated discs. Adams and Hutton[2] also observed this association. Several investigators, using plain radiographs, have concluded that disc degeneration and prolapse are strongly linked.[11,12,14] It is our belief that a similar comparison using MRI cannot be made, because the difference between Schneiderman's Grades 1 and 2 are not distinct enough.

We found no clear predictive value for nuclear extrusion or annular protrusion based on biomechanical disc characteristics. This again supports the belief that it is the load the disc experiences, and not the inherent quality of the disc that leads to prolapse.

CONCLUSION

A histologic review of surgical specimens has found annular material to be the overwhelming component in proven cases of disc prolapse.[29] Similarly, our investigation found a preponderance of annular deforma-

Table 7. Initial Stiffness (N/mm)

Specimen No.	Time (Minutes) 0	30	60	90	120	150	180	210	240	270	300	330	360	390
6	665	644	610	538	503	438	410	383	377	369	366	342	328	326
7	729	558	533	529	518	495	441	383	376	365	359	352	342	338
8*	859	681	492	553	513	NA	NA	NA	NA	NA	NA	NA	NA	330
9*	1852	1319	1267	1119	1134	1036	992	992	975	933	931	926	873	NA
10	1750	1458	1138	1050	1014	889	861	855	834	790	780	763	768	NA
11*	1601	1079	1000	839	804	796	760	738	656	650	646	602	596	NA
12	1837	1549	1520	1438	1368	1325	1167	1129	1086	1033	1033	958	945	932
13	1618	1225	1075	996	941	875	786	738	711	687	675	673	673	NA
14	328	291	269	255	201	NA	147	NA	NA	NA	NA	NA	NA	NA
Average	1249	978	878	813	777	836	696	745	716	690	684	659	646	481

*Nuclear extrusion.
NA = Not available.

Table 8. Final Stiffness (N/mm)

Specimen No.	Time (Minutes) 0	30	60	90	120	150	180	210	240	270	300	330	360	390
6	3111	3013	2823	2722	2656	2640	2625	2504	2386	2377	2363	2350	2346	2338
7	3824	3455	3208	3044	2992	2844	2799	2111	2352	2269	2258	2246	2240	2232
8*	2885	2728	2504	2678	2580	NA	NA	NA	NA	NA	NA	NA	NA	2059
9*	2941	2413	2074	1901	1756	1658	1575	1500	1370	1363	1277	1267	1260	NA
10	2940	2493	2333	2278	2210	2016	1925	1908	1844	1811	1804	1802	1763	NA
11*	2333	2228	1998	1758	1705	1688	1566	1539	1502	1496	1462	1459	1452	NA
12	2737	2445	2307	2218	2184	2163	2000	1985	1820	1788	1788	1637	1609	1556
13	2497	2238	2112	1805	1664	1706	1627	1351	1298	1295	1285	1272	1272	NA
14	1327	1064	949	933	843	NA	815	NA	NA	NA	NA	NA	NA	NA
Average	2732	2453	2256	2148	2066	2102	1866	1842	1796	1775	1748	1720	1706	2046

*Nuclear extrusion.
NA = Not available.

Table 9. Percentage of Stiffness Change Relative to the Stiffness at Time Zero

Specimen No.	Time (Minutes) 30	60	150	360
6	3.2%	8.2	34.2	50.7
7	23.5	26.9	32.1	53.1
8*	20.7	42.7	NA	NA
9*	29.0	37.8	44.1	52.9
10	16.7	35.0	49.2	56.1
11*	30.1	40.3	50.3	62.7
12	15.7	17.2	27.9	48.6
13	24.3	33.6	45.9	58.4
14	11.3	17.9	38.9	NA

*Nuclear extrusion.
NA = Not available.

Table 10. Final Stiffness Change Over Time

Specimen No.	Time (Minutes) 30	60	150	360
6	3.1%	9.3	15.1	24.6
7	9.7	16.1	25.6	41.4
8*	5.4	13.2	NA	NA
9*	21.7	31.0	43.6	57.2
10	15.2	20.7	30.2	40.0
11*	12.5	13.5	27.7	37.8
12	10.7	15.7	21	41.2
13	10.4	15.4	31.7	49.1
14	19.8	28.5	36.5	NA

*Nuclear extrusion.
NA = Not available.

Table 11. Energy Loss as a Function of Time

Specimen No.	Time (Minutes) 30	60	300
6	57.5 N-mm	82.6	65.7
7	52.7	78.5	53.9
8*	64.9	93.9	67.7
9*	47.5	85.8	66.7
10	40.6	79.1	58.1
11*	70.5	79.5	56.2
12	51.3	74.1	57.8
13	45.7	92.7	64.1
14	169.1	75.3	NA

*Nuclear extrusion.
NA = Not available.

tion and injury in the presence of contained nuclei. We contend that prolapse of the intervertebral disc is primarily the result of peripheral injury, namely annular disruption. We conclude that when the appropriate combination of flexion, rotation, and compression operate over an adequate length of time, annular separation and subsequent prolapse will occur.

REFERENCES

1. Adams MA, Hutton WC, Stott JRR: The resistance of flexion of the lumbar intervertebral joint. Spine 5:245–253, 1980
2. Adams MA, Hutton WC: Prolapsed intervertebral disc—A hyperflexion injury. Spine 7:184–191, 1982
3. Adams MA, Hutton WC: Gradual disc prolapse. Spine 7:184–191, 1982
4. Adams MA, Hutton WC: Has the lumbar spine a margin of safety in forward bending? Clin Biomech 1:3–6, 1986
5. Anderson GBJ, Schultz AB: Effects of fluid injection on mechanical properties of intervertebral discs. J Biomech 12:453–458, 1979
6. Brown T, Hansen RJ, Yorra AJ: Some mechanical tests on the lumbosacral spine with particular reference to the intervertebral discs. J Bone Joint Surg 39A:1135–1164, 1957
7. Chafetz NI, Genant HK, Moon KL, Helms CA, Morris JM: Recognition of lumbar disc herniation with NMR. AJR 141:1153–1156, 1983
8. Dandy WE: Loose cartilage from intervertebral disc simulating tumor of the spinal cord. Arch Surg 19:660–672, 1929
9. Eie N: Load capacity of the back. J Oslo City Hosp 16:73–98, 1966
10. Farfan HF, Cossette JW, Robertson GH, Wells RV, Krause H: The effects of torsion on the lumbar intervertebral joints: The role of torsion in the production of disc degeneration. J Bone Joint Surg 52A:468–497, 1970
11. Farfan HF: Mechanical Disorders of the Low Back. Philadelphia, Lea & Febiger, 1973, pp 16–35
12. Friberg S, Hirsch C: Anatomical and clinical studies on lumbar disc degeneration. Acta Orthop Scand 19:222–238, 1949
13. Galante JO: Tensile properties of the human lumbar annulus fibrosis. Acta Orthop Scand Suppl 100:94–101, 1967
14. Harris RI, McNab I: Structural changes in the lumbar intervertebral discs. J Bone Joint Surg 36B:304–322, 1954
15. Hickey DS, Hukins DWL: Relation between the structure of the annulus fibrosis and the function and failure of the intervertebral disc. Spine 5:106–115, 1980
16. Kelsey JL, Githens PB, O'Connor T, et al: Acute prolapsed lumbar intervertebral disc. Spine 9:608–613, 1984
17. Lin HS, Liu YK, Adams KH: Mechanical response of the lumbar intervertebral joint under physiologic (complex) loading. J Bone Joint Surg 60A:41–55, 1978
18. Liu YK, Goel VK, Dejong A, et al: Torsional fatigue of the lumbar intervertebral joints. Spine 10:894–900, 1985
19. Maravilla KR, Lesh P, Weinreb JC, Selby DK, Mooney V: Magnetic resonance imaging of the lumbar spine with CT correlation. Am J Neuroradiol 6:237–245, 1985
20. Nachemson AL, Schultz AB, Berkson MH: Mechanical properties of human lumbar spine motion segments. Spine 4:1–8, 1979
21. Norman D, Mills CM, Brant-Zawadzki M, et al: Magnetic resonance imaging of the spinal cord and canal: Potentials and limitations. AJR 141:1147–1152, 1983
22. Panjabi MM, Krag, Summers D, Videman T: Biomechanical time-tolerance of fresh cadaveric human spine specimens. J Orthop Res 3:292–300, 1985
23. Perey O: Fracture of the vertebral endplate. A biomechanical investigation. Acta Orthop Scand Suppl 25:588, 1957
24. Roaf R: A study of the mechanics of spinal injuries. J Bone Joint Surg 42B:810–823, 1960
25. Schneiderman G, Flannigan B, Kingston S, Thomas J, Dillin WH, Watkins RG: Magnetic resonance imaging in the diagnosis of disc degeneration: Correlation with discography. Spine 12:276–281, 1987
26. Smeathers JE, Joanes DN: Dynamic compressive properties of human lumbar intervertebral joints: A comparison between fresh and thawed specimens. J Biomech 21:425–433, 1988
27. Virgin WJ: Experimental investigations into the physical properties of the intervertebral disc. J Bone Joint Surg 33B:607–611, 1951
28. Yang KH, Byrd III AJ, Kish VL, Radin EL: Annulus fibrosus tears—An experimental model. Orthop Trans 12:86–87, 1988
29. Yasuma T, Makino E, Saito S, Inui M: Histologic development of intervertebral disc herniation. J Bone Joint Surg 68A:1066–1072, 1986

Address reprint requests to

Stuart J. Gordon, MD
Department of Orthopedic Surgery
West Virginia University
Morgantown, WV 26506

Accepted for publication September 28, 1990.